Science and Technology Indonesia
e-ISSN:2580-4391 *p*-ISSN:2580-4405
Vol. 8, No. 2, April 2023

Research Paper

Interlayer Modification of West Java Natural Bentonite as Hazardous Dye Rhodamine B Adsorption

Satria Jaya Priatna[1], Yusuf Mathiinul Hakim[2], Sahrul Wibyan[3], Siti Sailah[4], Risfidian Mohadi[1,2*]

[1]*Department of Soil Science, Sriwijaya University, Indralaya, 30862, South Sumatera, Indonesia*
[2]*Graduate School, Faculty of Mathematics and Natural Sciences, Sriwijaya University, Palembang, 30139, Indonesia*
[3]*Department of Chemistry, Faculty of Mathematics and Natural Sciences, Sriwijaya University, Indralaya, 30862, South Sumatera, Indonesia*
[4]*Department of Physics, Faculty of Mathematics and Natural Sciences, Sriwijaya University, Palembang, 30139, Indonesia*
***Corresponding author**: risfidian.mohadi@unsri.ac.id

Abstract
This work reports the modification of West Java natural bentonite as an effective adsorbent for rhodamine B dye. The modification was finished by sodium intercalation at room temperature to get low-energy preparation. Characterization of bentonite-modified adsorbent was used SEM, XRD, FTIR, and BET analysis. The material pore size and surface area were increased by 0.303 nm and 178.710 m^2/g on Na-bentonite. The adsorption mechanism conformed well with the Freundlich isotherm model and pseudo-second-order kinetics equations. The adsorption process by thermodynamic analysis was endothermic and advantageous. Under the optimum condition of pH 6 (confirmed by pHpzc), initial dye concentration of 125 mg/L, and the adsorbent dosage of 0.09 g for 65 minutes, the Na-bentonite has a larger adsorption capacity (Qm) of 142.86 mg/g, while the different adsorbent dosages of 0.11 g for 75 minutes, the adsorption capacity of natural bentonite (Qm) reaches 140.85 mg/g. This work provides a method for establishing a low-energy preparation adsorbent of bentonite-based on Na-intercalant as a low-cost and valuable adsorbent for waste dye removal.

Keywords
Bentonite, Intercalation, Low Temperature, Adsorption, Rhodamine B

Received: 3 October 2022, Accepted: 23 January 2023
https://doi.org/10.26554/sti.2023.8.2.160-169

1. INTRODUCTION

In recent years, environmental contamination has become a crucial issue due to the massive disposal of industrial waste (Asgari et al., 2021; Soleimani et al., 2022). Massive wastewater disposed of led to contamination in the ecosystem (Kamarehie et al., 2020; Rahmani et al., 2022). Coloring products are widely used in the food, cosmetics, pharmaceuticals, paints, and textiles industries (Laysandra et al., 2017). It was estimated that 7x105 tons of dye waste are produced annually (AL Tufaily and Al Qadi, 2016; Mohammad et al., 2019).

Rhodamine B (RhB) is a basic cationic dye with complex structures shown in Figure 1. In some cases, long-term exposure to RhB likely triggers temporary skin, and mucous membrane irritation, until the mutagenic effect (Laysandra et al., 2017). Several works provide techniques to detach the pollutants such as precipitation, osmotic reverse, flocculation/coagulation, electrodialysis, and adsorption (Dotto et al., 2019; Giraldo et al., 2022; Xie et al., 2022). Adsorption becomes the most efficient due to the organics, toxic metals, and dye contaminants binding to the solid adsorbent. Those stable contaminants bonded physically or chemically at the adsorbent surface (Chai et al., 2020; Mohammad et al., 2019). Potential low-cost adsorbents that provide adsorption features are zeolites, limestone, silica gel, chitosan, dolomite, activated carbon, and bentonite/clay.

Nowadays, the layered material of alumina-silicate bentonite has gained popularity as a low-cost adsorbent due to its abundance and high potency to enhance adsorbing capacity. The limitation of natural bentonite due to its rigid structure and the negative charge that is only sensitive to removing cationic dyes have encouraged researchers to modify the bentonite structure (Ding et al., 2018). However, the intercalation of natural bentonite by cationic exchange assisted by calcination to increase the adsorption capacity is favorable (Srikacha et al., 2022). However, the intercalation step may need a longer preparation time of 3 h to 10 days, moreover calcination process of more than 300°C to change the bentonite structure could trigger a collapse of the bentonite structure (Bouras et al., 2007; Leodopoulos et al., 2015). Recently, Islam and Mostafa

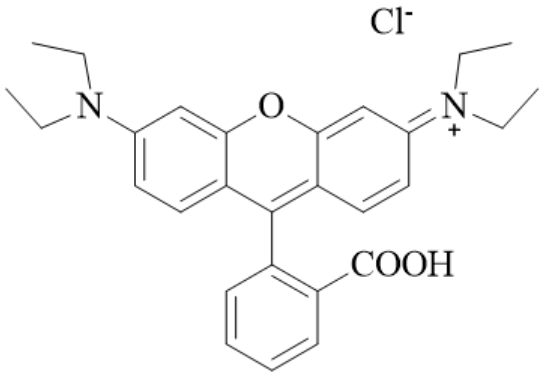

Figure 1. Chemical Structure of RhB Dye

(2022) studied the natural sodium bentonite adsorption capacity towards methylene blue by an adsorption capacity of 25.19 mg/g. According to Shattar and Foo (2022), activation bentonite assisted by sodium salt under heating of 70°C gives removal of methylene blue with an adsorption capacity of 318.38 mg/g.

The intercalation process becomes a challenge in bentonite modification. The rigid characteristics of the bentonite structure block the intercalation of another molecule. Sodium intercalation, as the preliminary step, becomes the favorable solution. The opening interlayer process to insert the intercalant need some energy that uses heat and pressure. High energy insertion is the challenge to discover a new method of the intercalating molecule to increase the interlayer bentonite. According to the report of Lin et al. (2007), intercalation via intermolecular force becomes an effective method for inserting molecules in low temperatures to decrease energy consumption.

This work aims to intercalate the West Java natural bentonite by saturated sodium salt solution under the natural ambiance of low-temperature preparation to get intramolecular force in inserting the intercalant and evaluate its removal capacity on RhB from aqueous solutions. Sodium salt was chosen because it is non-toxic to essential substances in the environment and has a high cationic exchange capacity in bentonite surfaces (Alexandru, 2011). The bentonite-modified characterization used SEM, XRD, FTIR, and BET to analyze physicochemical structural changes. The adsorption mechanism of RhB was carried out with optimization of the operational condition by pHpzc, variations in time, the dosage of adsorbent, temperature, and initial concentration.

2. EXPERIMENTAL SECTION

2.1 Chemicals and Instrumentation

The natural bentonite was obtained from West Java with purification. Chemicals in a pure grade, such as sodium chloride (NaCl), sodium hydroxide (NaOH), silver nitrate ($AgNO_3$), hydrochloric acid (HCl), and rhodamine B (RhB) dye, were purchased from Sigma-Aldrich and directly used without purification. Instrumentation such as X-Ray Diffractometer (XRD) type Rigaku Mini-flex600, Fourier Transfer Infra-Red (FTIR) type Perkin-Elmer UATR Spectrum two, UV-Vis Spectrophotometer type Orion AquaMate 8000, Scanning Electron Microscope Energy Dispersive Spectrometer (SEM-EDS) type JEOL JSM 6510-LA, and Surface Area Analyzer using Quantachrome ASIQ-win based on BET method calculation.

2.2 Bentonite Intercalation

The natural bentonite was modified by the cationic exchange methods at room temperature of 25°C: 100 g of natural bentonite dissolved in 333 mL of saturated NaCl and stirred for 2 hours. Then the mixture was added with distilled water (by two times the mixture volume) and continued stirring for 10 minutes. The bentonite mixture was precipitated and repeatedly added with 333 mL saturated NaCl, then mixed for 2 hours. It was washed three times with boiled distilled water, and the precipitate was oven-dried at 200°C for 12 hours. It is noticed as Na-bentonite.

2.3 Optimization of Operational Condition

The pHpzc (point zero charges) was determined by adding 0.02 g of adsorbent into 20 mL of 0.1 M NaCl solution and adjusted to pH of 2, 3, 4, 5, 6, 7, 8, 9, 10 using 0.1 M of NaOH and HCl solution. The mixture was stirred for 3 hours, and the final pH of the filtrate was measured using a pH meter to graph the pHpzc state.

2.4 Adsorption Studies

The effect of adsorption time was studied by varying the time adsorption at 5, 15, 25, 35, 45, 55, 65, 75, and 85 minutes. The composition of the adsorption process is 0.01 g of adsorbent into 50 mL of 30 mg/L RhB dyes. The effect of adsorbent dosages was studied by variation of adsorbent dosages at 0.01, 0.03, 0.05, 0.07, 0.09, 0.11, and 0.13 g. The effect of temperature and concentration adsorption was conducted on the adsorption of RhB using various temperatures and initial concentrations at 30, 40, 50, 60, and 70°C, with the concentration of RhB 25, 50, 75, 100, and 125 mg/L.

2.5 Analysis of Mechanism Adsorption

Adsorption kinetics of this experiment conducted by Wu et al. (2021) for pseudo-first order and pseudo-second order kinetic models are shown in Equation 1 and 2, respectively:

$$ln(qe - qt) = lnqe - tK_1 \quad (1)$$

$$\frac{t}{qt} = \frac{1}{q_e^2} + \frac{t}{qe} \quad (2)$$

Where K_1 is the rate constant of pseudo-first order (min^{-1}), K_2 is the constant rate of pseudo-second order ($g.mg^{-1}min^{-1}$), t for time, then qe and qt are capacity adsorption at equilibrium

and specific time, respectively. The Langmuir and Freundlich adsorption isotherm were analyzed to know the adsorption isotherm of this experiment according to Sahnoun et al. (2018) by the equation, respectively:

$$\frac{Ce}{qe} = \frac{1}{q_{max}K_L} + \frac{Ce}{q_{max}} \quad (3)$$

$$lnqe = lnK_F + \frac{lnC_e}{n} \quad (4)$$

Where qe is the capacity equilibrium of adsorbent (mg/g), Ce is the concentration equilibrium after adsorption (mg/L), q_{max} is the capacity maximum of adsorption (mg/g), K_L is constant of Langmuir adsorption (L/mg), then K_f and n are constant of Freundlich adsorption (L/g). Furthermore, the thermodynamic parameters can be analyzed by following equations (Dotto et al., 2019):

$$\Delta G = -RTlnK_d \quad (5)$$

$$\Delta G = \Delta H - T\Delta S \quad (6)$$

$$lnK_d = \frac{\Delta S}{R} - \frac{\Delta H}{RT} \quad (7)$$

Where ΔG° is the value of free energy Gibbs (kJ/mol), ΔH° is the enthalpy change of adsorption (kJ/mol), ΔS° is adsorption entropy change (kJ/mol.K), R is the standard gas constant (8.324 kJ/mol), T is temperature reaction (K), and K_d is the equilibrium constant.

3. RESULT AND DISCUSSION

3.1 Characterization of Adsorbents

The morphologies of modified bentonite were observed using SEM techniques in Figure 2 shows a massive quantity of lamellar particles with unshaped aggregated and rough particles attached to the surface area, especially in modified bentonite in Figure 2b (Mahmoodi, 2015). Aggregate and rough particles may be impurities from zeolite, while according to Figure 2a, the flake's structures are considered montmorillonite(Jiang et al., 2021). According to Figure 2b, lamellar structures in Na-bentonite present numerous small particles attached. Those phenomena showed that cation exchange significantly reduced impurities, confirmed by detailed EDX data in Table 1. The intercalation process affected the removal of the Ti substance.

The composition and structural changes are reflected by XRD analysis in Figure 3. The basal spacing of the bentonite-modified adsorbents is 8.06 nm and corresponds to the d001 peak, the value of 2θ about 20°, noticed as montmorillonite.

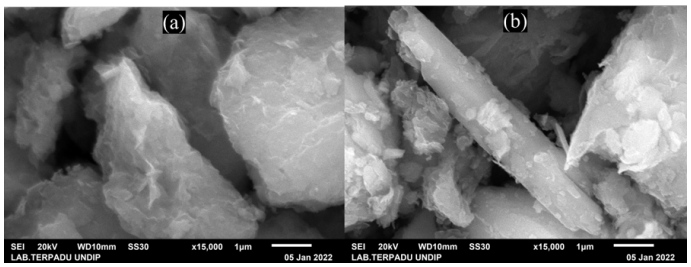

Figure 2. SEM Image of (a) Natural Bentonite (b) Na-bentonite

The sodium-intercalated did not change significantly due to low interaction binding and the size particle of sodium identic to the previous cation in the interlayer. Unfortunately, the sodium intercalation has affected the cationic exchange, and it is confirmed from Figure 3 that the peak positions of all adsorbents are similar (He et al., 2022). According to the data of XRD, the crystal size of natural bentonite and Na-bentonite are 4.35 nm and 8.06 nm, respectively. Modifying bentonite assisted by sodium intercalation between interlayers increases the montmorillonite composition, layer space, and adsorption capacity by providing the cationic exchange field. According to JCPDS data No. 24-0495 shows that 2θ at around 20°, 35°, 55°, and 63° are montmorillonite compounds. Then, for 2θ at about 26° are quartz compounds, while at 2θ around 28° are compounds composed of Al, Si, and O (Reza et al., 2015).

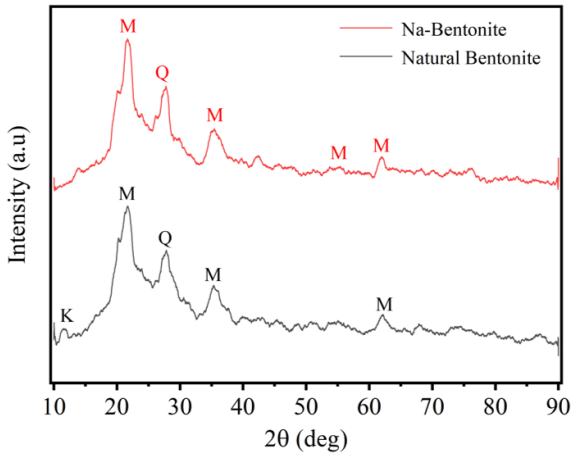

Figure 3. XRD Patterns of (a) Natural Bentonite and (b) Na-bentonite

Bentonite, as layered material, has several functional groups that influence adsorption. The FT-IR spectrums of bentonite-modified are displayed in Figure 4. The composition of OH octahedra stretching vibrations at the surface layer is indicated by a peak at 3380 cm^{-1} . A peak indicates the H-O-H vibrations of the water molecule at 1632 cm^{-1} . The layer structures of bentonite were confirmed by stretching vibrations of Si-O-

Table 1. EDX Data of Bentonite-modified Adsorbent

Element	Natural bentonite (%W)	Na-bentonite (%W)
O	57.88	54.83
Si	22.17	22.86
C	13.02	10.77
Al	3.32	4.21
Fe	1.34	1.42
Mg	0.71	0.69
Cu	0.62	1.10
Ca	0.27	1.59
K	0.26	0.48
Na	0.23	0.84
Ti	0.17	-

Table 2. The Analysis of BET Surface Area, Pore Diameter, and Pore Volume of the Natural Bentonite and Na-bentonite

Adsorbent	BET Surface Area (m^2/g)	Pore Diameter (nm)	Pore Volume (cm^3/g)
Natural bentonite	61.791	4.678	0.144
Na-bentonite	178.710	3.401	0.303

Si from the peak at 1028 cm^{-1} and vibrations of Al-O-Al from the peak at 791 cm^{-1} (Castellini et al., 2017). The peak at 518 and 459 cm^{-1} is ascribed to the cation vibration on the layer structure of bentonite. The difference in peak sharpness affected vibration intensity due to sodium salt intercalant power binding at the surface interlayers, thus giving additional functional groups between interlayers (Yang et al., 2022).

The textural characteristics of natural bentonite and the intercalated one were characterized via the N_2 adsorption-desorption method at 77.35 K. Detailed result was plotted in the graph of N_2 adsorption-desorption isotherm characteristics in Figure 5. The isotherm trend from the natural bentonite and Na-bentonite behave in the same condition that fits into the type IV according to Braunnauer-Deming-Deming-Teller (BDTT) classification (Mu'azu et al., 2018). The overlapping of adsorption-desorption points occurred at the low relative pressure; thus fit with the H3 type of hysteresis loop that initiated at a relative pressure (P/P0) around 0.42. The emerging features are grouped as the characteristic of the mesopore layered material (Tong et al., 2018; Yurdakal et al., 2019).

The precise surface area value calculated using the BET model on natural and Na-bentonite is tabulated in Table 2. In this case, the specific surface area of bentonite-intercalated Na^+ was differently higher than the natural one. It assumed that sodium intercalations' effectivity significantly impacts the active surface of adsorbent-adsorbate interaction in multiple quantities and generates additional mesopores (Javed et al., 2018). Despite the decreasing pore diameter, the pore volume was increasing due to the enormous size of intercalate, thus promoting the adsorption process (Ain et al., 2020; Mohammed and Isra'a, 2018).

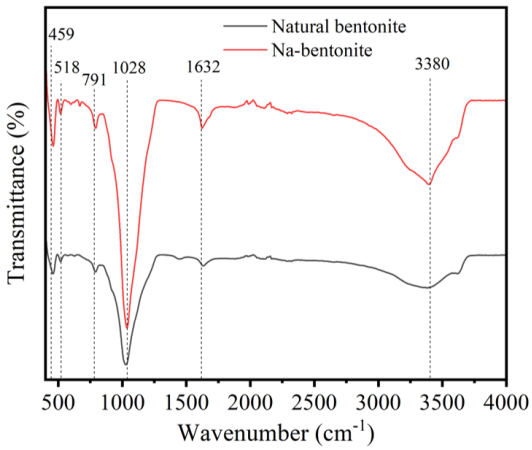

Figure 4. FT-IR Spectrums of (a) Natural Bentonite and (b) Na-bentonite

3.2 Optimization of Operational Conditions

The pHpzc of bentonite-based adsorbent was plotted by Al Maliky et al. (2021) in Figure 6, which turned out to be 4.35 for natural bentonite and 5 for Na-bentonite provides an acid medium for adsorption of dyes. The role of pHpzc is to determine the influence of pH range on the active site of the surface adsorbent. The value of pH > pHpzc induces optimum adsorption of cationic dyes due to negative charge increases on adsorbent (Kanwal et al., 2022). RhB has a positive charge in the solvent, then tends to adsorb at a higher pH value than the pHpzc condition (Ribeiro dos Santos et al., 2019). It is appropriate for the experiment due to the optimum adsorption

Table 3. Adsorption Kinetic Model

Model Kinetics Adsorption	Parameter	Adsorbent Natural bentonite	Adsorbent Na-bentonite
Pseudo First Order	Qe (mg/g)	102.49	119.22
	k_1	0.062	0.058
	R^2	0.926	0.883
Pseudo Second Order	Qe (mg/g)	102.49	102.49
	k_2	0.006	0.007
	R^2	0.9975	0.9978

Table 4. Parameter of Isotherm Adsorption of RhB on the Bentonite-modified Adsorbent

Adsorbent	Isotherm Model	Parameter Adsorption	Temperature (°C)				
			30	40	50	60	70
Natural Bentonite	Langmuir	Qm	140.85	133.33	138.89	125	123.46
		KL	0.023	0.033	0.034	0.057	0.114
		R^2	0.930	0.913	0.914	0.919	0.809
	Freundlich	n	1.506	1.641	1.647	1.808	2.244
		KF	4.827	6.193	6.427	7.984	12.159
		R^2	0.995	0.991	0.991	0.987	0.946
Na-bentonite	Langmuir	Qm	142.86	136.99	140.85	138.89	140.85
		KL	0.035	0.054	0.063	0.078	0.107
		R^2	0.972	0.994	0.994	0.991	0.994
	Freundlich	n	1.536	1.648	1.687	1.720	1.783
		KF	5.725	7.037	7.628	8.093	8.978
		R^2	0.993	0.998	0.997	0.996	0.997

of RhB occurring at pH 6 based on preliminary laboratory screening.

3.3 Effect of Adsorption Time

The effect of variations in the contact time of bentonite-based adsorbent on RhB is seen in Figure 7. Figure 7 shows that the equilibrium adsorption time of RhB on natural bentonite reaches 75 minutes, while the equilibrium time on Na-bentonite reaches 65 minutes. According to the literature, the calculated data of adsorption was gained using pseudo-first-order (PFO) and pseudo-second-order (PSO) kinetic equations (Mohadi et al., 2022). The results of kinetic data adsorption on variation time adsorption are shown in Table 3.

Based on Table 3, the kinetic data shows that the linear regression value (R^2) of the pseudo-second-order (PSO) tends to be closer to 1 value than to the pseudo-first-order (PFO) kinetic model, so it concluded that RhB adsorption in bentonite-based adsorbent follows the PSO model kinetics. It suggested that adsorption tends to occur by chemisorption, then the adsorption equilibrium rate is affected by the adsorbent and adsorbate composition (Shattar and Foo, 2022).

3.4 Effect of Adsorbent Dosage

Effect of variation dosages adsorption was prepared under room temperatures, pH = 6, adsorption time of 65 minutes for natural bentonite and 75 minutes for Na-bentonite. Figure 8 shows the adsorption rate for 30 mg/L RhB with a variation of bentonite-modified adsorbent dosages, where variation dosages were used from 0.01, 0.03, 0.05, 0.07, 0.09, 0.11, and 0.13 g. Based on Figure 8, the equilibrium of adsorption rate of the natural bentonite and Na-bentonite occurred at 0.11 g and 0.09 g, respectively, with insignificant increases at adsorbent dosages of more than 0.11g. The insignificant increase is related to the restricted concentration of dye that can be adsorbed and the agglomeration in bentonite adsorbent (Khan et al., 2012).

3.5 Effect of Concentration and Adsorption Temperature

According to Figure 9, the increases in adsorption temperature will cause a decrease in the adsorbate adsorbed for the RhB dye. Otherwise, the concentration increases are affected by RhB adsorbed. Data in Tables 4 and 5 were used to determine the adsorption isotherm model using the Langmuir and Freundlich equation based on (Sahnoun et al., 2018). The data of the Langmuir and Freundlich isotherm calculation are shown in Table 4.

According to Huang et al. (2017), the Langmuir isotherm model ascribed that adsorption occurs by the monolayer conformation on the surface of the adsorbent, thus not having interactions between molecules of adsorbate, while the Freundlich

Table 5. Adsorption Thermodynamic Parameter Data on Natural Bentonite

Consentration (mg/L)	Temperature (K)	Qe (mg/g)	ΔH (kJ/mol)	ΔS (J/K.mol)	ΔG (kJ/mol)
	303	18.188			-2.218
	313	19.233			-2.917
25	323	19.442	18.96	0.070	-3.616
	333	20.278			-4.315
	343	22.055			-5.014
	303	31.568			-1.348
	313	32.892			-1.599
50	323	33.380	6.24	0.025	-1.849
	333	34.147			-2.099
	343	34.983			-2.350
	303	45.784			-1.117
	313	46.411			-1.259
75	323	47.038	3.19	0.014	-1.401
	333	47.874			-1.543
	343	48.293			-1.685
	303	58.536			-0.877
	313	60.487			-1.062
100	323	61.463	4.72	0.018	-1.246
	333	62.299			-1.431
	343	64.111			-1.616
	303	69.861			-0.590
	313	71.777			-0.740
125	323	72.823	3.95	0.015	-0.890
	333	73.171			-1.039
	343	76.133			-1.189

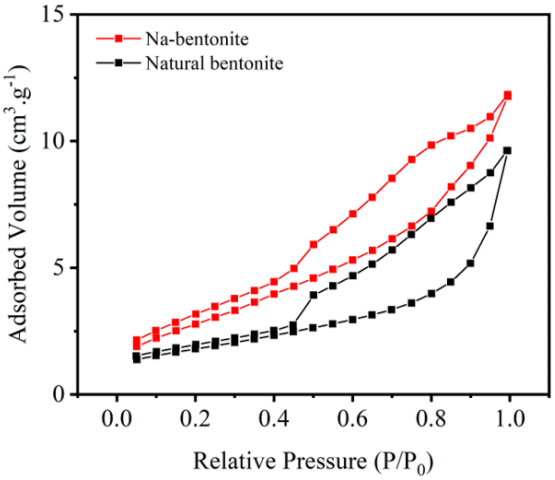

Figure 5. N_2 Adsorption-Desorption Properties

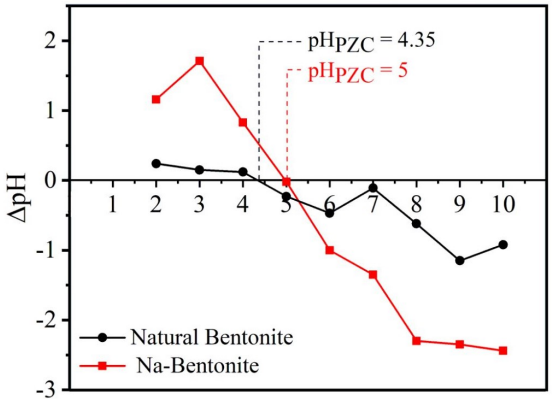

Figure 6. The pHpzc of (a) Natural Bentonite and (b) Na-bentonite

isotherm ascribed that the adsorbent is supported multilayer and heterogeneous adsorption, thus adsorption process occurs by physical. Based on Table 4, the Freundlich isotherm model shows a linear regression value (R^2) closer to the value 1 than the Langmuir isotherm model for RhB adsorption, indicating that RhB adsorptions are spread heterogeneously (Xing et al., 2015). The dimensions of the exponent 1/n state the favorable interaction between adsorbent-adsorbate. Adsorption will be beneficial if n > 1. In this study, the adsorption of RhB is easy due to an n value higher than 1 (Annadurai et al., 2000).

Furthermore, according to Huang et al. (2017) calculation

Table 6. Adsorption Thermodynamic Parameter Data on Na-Bentonite

Concentration (mg/L)	Temperature (K)	Qe (mg/g)	ΔH (kJ/mol)	ΔS (J/K.mol)	ΔG (kJ/mol)
	303	18.710			-2.747
	313	19.616			-3.131
25	323	19.965	8.88	0.038	-3.515
	333	20.174			-3.898
	343	20.627			-4.282
	303	43.742			-2.094
	313	44.648			-2.379
50	323	44.997	6.54	0.028	-2.664
	333	45.206			-2.949
	343	45.659			-3.234
	303	49.861			-1.720
	313	50.592			-1.893
75	323	51.428	3.50	0.017	-2.065
	333	51.951			-2.237
	343	52.474			-2.410
	303	61.324			-1.188
	313	62.996			-1.328
100	323	63.554	3.06	0.014	-1.468
	333	63.972			-1.609
	343	64.947			-1.749
	303	72.474			-0.822
	313	74.216			-0.964
125	323	75.610	3.47	0.014	-1.105
	333	76.133			-1.247
	343	77.526			-1.388

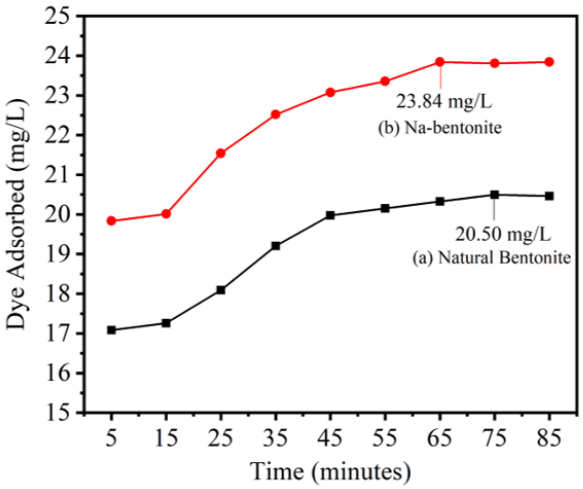

Figure 7. Effect of Contact Time Adsorption on (a) Natural Bentonite and (b) Na-bentonite

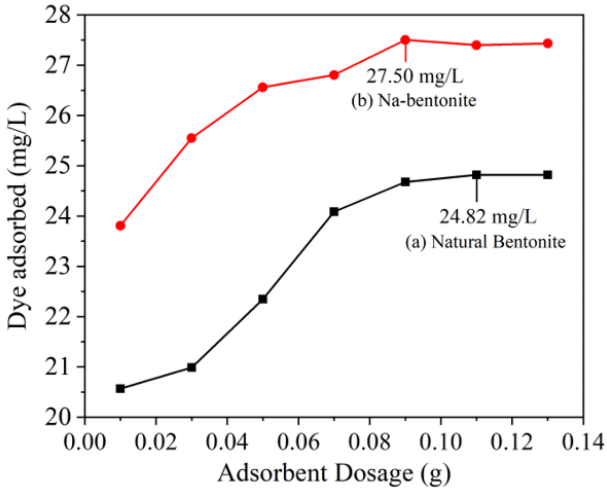

Figure 8. Effect of Adsorbent Dosage on (a) Natural Bentonite and (b) Na-bentonite

Table 7. Comparative of Adsorption Capacity on Rhodamine B in Different Adsorbent

Bentonite	Adsorbate	Adsorption Capacity (mg/g)	Optimum Time (minutes)	References
Na-bentonite	RhB	142.86	65	This study
Bentonite-CTA-DAPTMS	RhB	0.98	5	de Morais Pinos et al. (2022)
γ- Fe_2O_3/montmorillonite	RhB	45.08	60	Fatimah et al. (2022)
Beta zeolite SiO_2/Al_2O_3	RhB	27.97	60	Cheng et al. (2018)
α-Al_2O_3	RhB	52	30	Yen Doan et al. (2020)

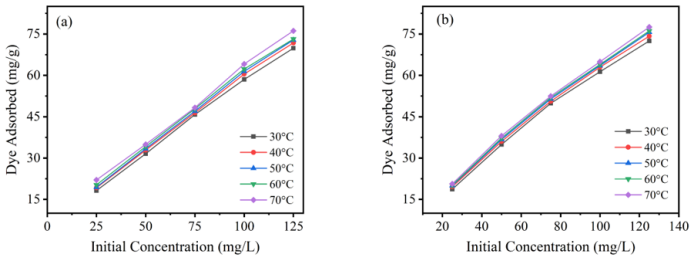

Figure 9. Effect of Temperature and Concentration Adsorption of RhB on (a) Natural Bentonite and (b) Na-bentonite

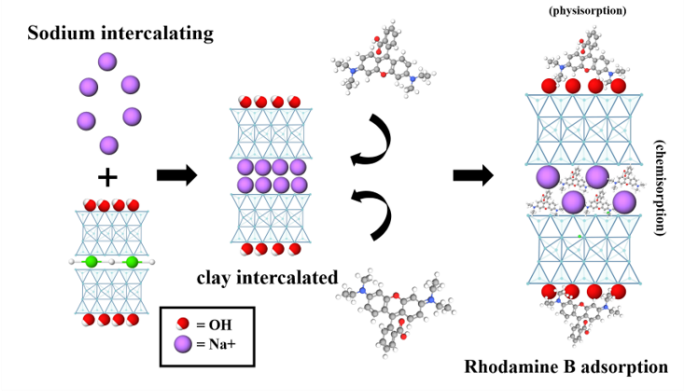

Figure 10. Mechanism Interaction Proposed of RhB Adsorption Bentonite-modified

of thermodynamic parameters can provide data (ΔG°), (ΔS°), and (ΔH°). The detail of the thermodynamic parameter data is shown in Tables 4 and 5 . The calculation results for ΔG° value are negative on each adsorbent; thus, the value decreased with increasing adsorption temperature. A negative value of ΔG° indicates that the RhB adsorption process is beneficial and spontaneously occurs He et al. (2022), and the adsorption is better at high temperatures. The ΔH° value showed a range of 18.96 kJ/mol to 3.95 kJ/mol was related to the tendency of RhB adsorption to occur by physical adsorption and endothermic based on a positive ΔH° value, thus supporting the isotherm adsorption analysis. The adsorption mechanism of RhB into bentonite-modified adsorbent visualized in Figure 10. Physisorption as dominant mechanism take a apart in bentonite negative charge of surface, then the cation exchange of RhB into interlayer bentonite has reduce the sodium ion in the interlayer structure (Selvam et al., 2008). Another result is the positive value of ΔS°, which is related to the irregularity of the particles during adsorption increases due to the adsorbent-liquid interaction between the bentonite-based adsorbent and RhB (Mahmoodi, 2014).

4. CONCLUSION

In summary, the new route modification of natural bentonite imported from West Java of Indonesia was completed using cation exchange of sodium salt-intercalant under low room temperature of 25°C to develop efficient and low energy prepared adsorbent to remove RhB dyes in an aqueous solution. The bentonite-modified was characterized by several characterization techniques, indicating the sodium was intercalated on the interlayer bentonite. The adsorption study proved that Na-bentonite effectively removed the RhB with adsorption capacity (Qm) reached 142.86 mg/g for Na-bentonite by physisorption and spontaneously endothermic occurred.

5. ACKNOWLEDGMENT

The research of this article was funded by DIPA of Public Service Agency of Universitas Sriwijaya 2022. SP DIPA-23.17.2.677515 /2022, On Desember 13, 2021. Under the Rectors Decree 0017/UN9.3. 1 /SK.LP2M.PT/2022, On Juni 15, 2022.

REFERENCES

Ain, Q. U., U. Rasheed, M. Yaseen, H. Zhang, R. He, and Z. Tong (2020). Fabrication of Magnetically Separable 3-acrylamidopropyltrimethylammonium Chloride Intercalated Bentonite Composite for the Efficient Adsorption of Cationic and Anionic Dyes. *Applied Surface Science*, **514**; 145929

Al Maliky, E. A., H. A. Gzar, and M. G. Al Azawy (2021). Determination of Point of Zero Charge (PZC) of Concrete Particles Adsorbents. *IOP Conference Series: Materials Science and Engineering*, **1184**(1); 012004

AL Tufaily, M. and Z. Al Qadi (2016). Preparation and Utilization of Corncob Activated Carbon for Dyes Removal from Aqueous Solutions: Batch and Continuous Study. *Journal of Babylon University/Engineering Sciences*, **2**(3); 24

Alexandru, I. (2011). The Role Of Sodium In the Body Stantin. *In Balneo-Research Journal*, **2**(3); 23–25

Annadurai, G., S. Rajesh Babu, K. Mahesh, and T. Murugesan (2000). Adsorption and Bio-degradation of Phenol by Chitosan-immobilized Pseudomonas Putida (NICM 2174). *Bioprocess Engineering*, **22**(6); 493–501

Asgari, G., A. Seid Mohammadi, A. Rahmani, M. T. Samadi, M. Salari, S. Alizadeh, and D. Nematollahi (2021). Diuron Degradation using Three-dimensional Electro-peroxone (3D/E-peroxone) Process in the Presence of TiO2/GAC: Application for Real Wastewater and Optimization using RSM-CCD and ANN-GA Approaches. *Chemosphere*, **266**; 129179

Bouras, O., J. C. Bollinger, M. Baudu, and H. Khalaf (2007). Adsorption of Diuron and its Degradation Products from Aqueous Solution by Surfactant-modified Pillared Clays. *Applied Clay Science*, **37**(3-4); 240–250

Castellini, E., D. Malferrari, F. Bernini, M. F. Brigatti, G. R. Castro, L. Medici, A. Mucci, and M. Borsari (2017). Baseline Studies of the Clay Minerals Society Source Clay Montmorillonite STx-1b. *Clays and Clay Minerals*, **65**(4); 220–233

Chai, J. B., P. I. Au, N. M. Mubarak, M. Khalid, W. P. Q. Ng, P. Jagadish, R. Walvekar, and E. C. Abdullah (2020). Adsorption of Heavy Metal from Industrial Wastewater Onto Low-cost Malaysian Kaolin Clay–based Adsorbent. *Environmental Science and Pollution Research*, **27**(12); 13949–13962

Cheng, Z. L., Y. x. Li, and Z. Liu (2018). Study on Adsorption of Rhodamine B Onto Beta Zeolites by Tuning SiO2/Al2O3 Ratio. *Ecotoxicology and Environmental Safety*, **148**; 585–592

de Morais Pinos, J. Y., L. B. de Melo, S. D. de Souza, L. Marçal, and E. H. de Faria (2022). Bentonite Functionalized with Amine Groups by the Sol-gel Route as Efficient Adsorbent of Rhodamine-B and Nickel (II). *Applied Clay Science*, **223**; 106494

Ding, F., M. Gao, T. Shen, H. Zeng, and Y. Xiang (2018). Comparative Study of Organo-vermiculite, Organo-montmorillonite and Organo-silica Nanosheets Functionalized by An Ether-spacer-containing Gemini Surfactant: Congo Red Adsorption and Wettability. *Chemical Engineering Journal*, **349**; 388–396

Dotto, J., M. R. Fagundes-Klen, M. T. Veit, S. M. Palacio, and R. Bergamasco (2019). Performance of Different Coagulants In the Coagulation/flocculation Process of Textile Wastewater. *Journal of Cleaner Production*, **208**; 656–665

Fatimah, I., G. Purwiandono, A. Hidayat, S. Sagadevan, and A. Kamari (2022). Mechanistic Insight Into the Adsorption and Photocatalytic Activity of a Magnetically Separable γ-Fe2O3/Montmorillonite Nanocomposite for Rhodamine B Removal. *Chemical Physics Letters*, **792**; 139410

Giraldo, S., N. Y. Acelas, R. Ocampo Pérez, E. Padilla Ortega, E. Flórez, C. A. Franco, F. B. Cortés, and A. Forgionny (2022). Application of Orange Peel Waste as Adsorbent for Methylene Blue and Cd2+ Simultaneous Remediation. *Molecules*, **27**(16); 5105

He, H., K. Chai, T. Wu, Z. Qiu, S. Wang, and J. Hong (2022). Adsorption of Rhodamine B from Simulated Waste Water onto Kaolin-Bentonite Composites. *Materials*, **15**(12); 4058

Huang, Z., Y. Li, W. Chen, J. Shi, N. Zhang, X. Wang, Z. Li, L. Gao, and Y. Zhang (2017). Modified Bentonite Adsorption of Organic Pollutants of Dye Wastewater. *Materials Chemistry and Physics*, **202**; 266–276

Islam, M. and M. Mostafa (2022). Adsorption Kinetics, Isotherms and Thermodynamic Studies of Methyl Blue in Textile Dye Effluent on Natural Clay Adsorbent. *Sustainable Water Resources Management*, **8**(2); 1–12

Javed, S. H., A. Zahir, A. Khan, S. Afzal, and M. Mansha (2018). Adsorption of Mordant Red 73 Dye on Acid Activated Bentonite: Kinetics and Thermodynamic Study. *Journal of Molecular Liquids*, **254**; 398–405

Jiang, K., K. Liu, Q. Peng, and M. Zhou (2021). Adsorption of Pb (II) and Zn (II) Ions on Humus-like Substances Modified Montmorillonite. *Colloids and Surfaces A: Physicochemical and Engineering Aspects*, **631**; 127706

Kamarehie, B., A. Jafari, M. Ghaderpoori, F. Azimi, M. Faridan, K. Sharafi, F. Ahmadi, and M. A. Karami (2020). Qualitative and Quantitative Analysis of Municipal Solid Waste In Iran For Implementation of Best Waste Management Practice: A Systematic Review and Meta-analysis. *Environmental Science and Pollution Research*, **27**(30); 37514–37526

Kanwal, A., R. Rehman, and M. Imran (2022). Adsorptive Detoxification of Congo Red and Brilliant Green Dyes Using Chemically Processed Brassica Oleracea Biowaste from Waste Water. *Adsorption Science & Technology*, **2022**; 1–14

Khan, T. A., S. Dahiya, and I. Ali (2012). Use of Kaolinite as Adsorbent: Equilibrium, Dynamics and Thermodynamic Studies on the Adsorption of Rhodamine B From Aqueous Solution. *Applied Clay Science*, **69**; 58–66

Laysandra, L., M. W. M. K. Sari, F. E. Soetaredjo, K. Foe, J. N. Putro, A. Kurniawan, Y. H. Ju, and S. Ismadji (2017). Adsorption and Photocatalytic Performance of Bentonite-titanium Dioxide Composites for Methylene Blue and Rhodamine B Decoloration. *Heliyon*, **3**(12); e00488

Leodopoulos, C., D. Doulia, and K. Gimouhopoulos (2015). Adsorption of Cationic Dyes Onto Bentonite. *Separation & Purification Reviews*, **44**(1); 74–107

Lin, J. J., Y. M. Chen, and M. H. Yu (2007). Hydrogen-bond Driven Intercalation of Synthetic Fluorinated Mica by Poly (oxypropylene)-amidoamine Salts. *Colloids and Surfaces A: Physicochemical and Engineering Aspects*, **302**(1-3); 162–167

Mahmoodi, N. M. (2014). Dendrimer Functionalized Nanoarchitecture: Synthesis and Binary System Dye Removal. *Journal of the Taiwan Institute of Chemical Engineers*, **45**(4); 2008–2020

Mahmoodi, N. M. (2015). Manganese Ferrite Nanoparticle: Synthesis, Characterization, and Photocatalytic Dye Degradation Ability. *Desalination and Water Treatment*, **53**(1); 84–90

Mohadi, R., E. S. Fitri, and N. R. Palapa (2022). Unique Adsorption Properties of Cationic Dyes Malachite Green and Rhodamine-B on Longan (Dimocarpus Longan) Peel.

Science and Technology Indonesia, **7**(1); 115–125

Mohammad, A. T., A. S. Abdulhameed, and A. H. Jawad (2019). Box-Behnken Design to Optimize the Synthesis of New Crosslinked Chitosan-glyoxal/TiO2 Nanocomposite: Methyl Orange Adsorption and Mechanism Studies. *International Journal of Biological Macromolecules*, **129**; 98–109

Mohammed, A. A. and S. S. Isra'a (2018). Bentonite Coated with Magnetite Fe3O4 Nanoparticles as A Novel Adsorbent for Copper (ii) Ions Removal From Water/wastewater. *Environmental Technology & Innovation*, **10**; 162–174

Mu'azu, N. D., N. Jarrah, T. S. Kazeem, M. Zubair, and M. Al Harthi (2018). Bentonite-layered Double Hydroxide Composite for Enhanced Aqueous Adsorption of Eriochrome Black T. *Applied Clay Science*, **161**; 23–34

Rahmani, A. R., N. Navidjouy, M. Rahimnejad, S. Alizadeh, M. R. Samarghandi, and D. Nematollahi (2022). Effect Of Different Concentrations of Substrate In Microbial Fuel Cells Toward Bioenergy Recovery and Simultaneous Wastewater Treatment. *Environmental Technology*, **43**(1); 1–9

Reza, E. M., J. P. Bueno, F. E. Arreola, L. A. Arellano, J. P. Robles, R. N. Mendoza, and A. H. Macías (2015). Organobentonites with Crystalline Layer Separation Used for Adsorption In Water Treatment. *Handbook of Research on Diverse Applications of Nanotechnology in Biomedicine, Chemistry, and Engineering*, **3**; 496–517

Ribeiro dos Santos, F., H. C. de Oliveira Bruno, and L. Zelayaran Melgar (2019). Use of Bentonite Calcined Clay As An Adsorbent: Equilibrium and Thermodynamic Study of Rhodamine B Adsorption In Aqueous Solution. *Environmental Science and Pollution Research*, **26**(28); 28622–28632

Sahnoun, S., M. Boutahala, C. Tiar, and A. Kahoul (2018). Adsorption of Tartrazine From An Aqueous Solution by Octadecyltrimethylammonium Bromide-modified Bentonite: Kinetics and Isotherm Modeling. *Comptes Rendus Chimie*, **21**(3-4); 391–398

Selvam, P. P., S. Preethi, P. Basakaralingam, N. Thinakaran, A. Sivasamy, and S. Sivanesan (2008). Removal of Rhodamine B from Aqueous Solution by Adsorption Onto Sodium Montmorillonite. *Journal of Hazardous Materials*, **155**(1-2); 39–44

Shattar, S. F. A. and K. Y. Foo (2022). Sodium Salt-assisted Low Temperature Activation of Bentonite For the Adsorptive Removal of Methylene Blue. *Scientific Reports*, **12**(1); 1–12

Soleimani, H., O. Nasri, M. Ghoochani, A. Azhdarpoor, M. Dehghani, M. Radfard, M. Darvishmotevalli, V. Oskoei, and M. Heydari (2022). Groundwater Quality Evaluation and Risk Assessment of Nitrate Using Monte Carlo Simulation and Sensitivity Analysis In Rural Areas of Divandarreh County, Kurdistan Province, Iran. *International Journal of Environmental Analytical Chemistry*, **102**(10); 2213–2231

Srikacha, N., M. Sriuttha, L. Neeratanaphan, C. Saiyasombat, and B. Tengjaroensakul (2022). The Improvement of Natural Thai Bentonite Modified with Cationic Surfactants on Hexavalent Chromium Adsorption from an Aqueous Solution. *Adsorption Science & Technology*, **2022**; 1–15

Tong, D. S., C. W. Wu, M. O. Adebajo, G. C. Jin, W. H. Yu, S. F. Ji, and C. H. Zhou (2018). Adsorption of Methylene Blue From Aqueous Solution Onto Porous Cellulose-derived Carbon/montmorillonite Nanocomposites. *Applied Clay Science*, **161**; 256–264

Wu, Z., W. Deng, S. Tang, E. Ruiz Hitzky, J. Luo, and X. Wang (2021). Pod-inspired MXene/porous Carbon Microspheres with Ultrahigh Adsorption Capacity Towards Crystal Violet. *Chemical Engineering Journal*, **426**; 130776

Xie, L. Q., X. Y. Jiang, and J. G. Yu (2022). A Novel Low-Cost Bio-Sorbent Prepared from Crisp Persimmon Peel by Low-Temperature Pyrolysis for Adsorption of Organic Dyes. *Molecules*, **27**(16); 5160

Xing, X., G. Lv, W. Zhu, C. He, L. Liao, L. Mei, Z. Li, and G. Li (2015). The Binding Energy Between the Interlayer Cations and Montmorillonite Layers and Its Influence On Pb2+ Adsorption. *Applied Clay Science*, **112**; 117–122

Yang, D., F. Cheng, L. Chang, and D. Wu (2022). Sodium Modification of Low Quality Natural Bentonite as Enhanced Lead Ion Adsorbent. *Colloids and Surfaces A: Physicochemical and Engineering Aspects*, **651**; 129753

Yen Doan, T. H., T. P. Minh Chu, T. D. Dinh, T. H. Nguyen, T. C. Tu Vo, N. M. Nguyen, B. H. Nguyen, and T. D. Pham (2020). Adsorptive Removal of Rhodamine B Using Novel Adsorbent-based Surfactant-modified Alpha Alumina Nanoparticles. *Journal of Analytical Methods in Chemistry*, **2020**; 1–8

Yurdakal, S., C. Garlisi, L. Özcan, M. Bellardita, and G. Palmisano (2019). (Photo) Catalyst Characterization Techniques: Adsorption Isotherms and BET, SEM, FTIR, UV–Vis, Photoluminescence, and Electrochemical Characterizations. *Heterogeneous Photocatalysis*, **4**; 87–152

